Powder Metallurgy and Metal Ceramics, Vol. 51, Nos. 1-2, May, 2012 (Russian Original Vol. 51, Jan.-Feb., 2012)

THEORY AND TECHNOLOGY OF FORMING PROCESS

EFFECT OF MOLECULAR INTERACTION ON THE STRENGTH OF GREEN COMPACTS

O. K. Radchenko[1]

UDC 621.762.4

Modern approaches to calculating the strength of green compacts by van der Waals forces (σ_{VW}) are reviewed. Respective components (σ_{VW}) are calculated and green tensile strength ($\sigma_{tl.av}$) is experimentally determined for test powders of metals (Al, Zn, Cu, Ni, and Mo) and one nonmetal (FeSi). Comparison of $\sigma_{tl.av}/\sigma_{VW}$ ratios shows that $\sigma_{tl.av}$ and σ_{VW} are of one order for the atomized zinc powder, and σ_{VW} is greater than $\sigma_{tl.av}$ for the atomized copper powder, though $\sigma_{tl.av}$ is greater than σ_{VW} by two to three orders for most powders with irregular shape of particles. This difference can be attributed to the effect of shape and mechanical interlocking or seizure of particles when compacted. To predict the green strength, it is necessary to take into account both the shape of particles (or relative apparent density of the powder) and the forming temperature.

***Keywords**: green strength, van der Waals forces, particle shape, powders, relative apparent density, forming temperature.*

INTRODUCTION

The nature of green strength is still to be understood. In particular, the contribution of different components to strength yet remains to be determined [1]. Bonds between individual particles are considered to result from adhesion or self-adhesion interaction [2, 3]. Pietsch [2] mainly considered forces associated with van der Waals, electrostatic, and magnetic interaction. Zimon and Andrianov [3] calculated the self-adhesion force (F_1) as a sum of the following components:

$$F_1 = F_m + F_c + F_e + F_{mech} - F_{e.a}, \tag{1}$$

where F_m, F_c, F_e, F_{mech}, and $F_{e.a}$ are van der Waals, cohesion,* electric, mechanical, and elastic aftereffect forces.

The green strength can be divided into the molecular or van der Waals (σ_{VW}), mechanical (σ_{mech}), electrostatic (σ_{el}), chemical (σ_{chem}) [4], magnetic (σ_{mag}), and elastic aftereffect ($\sigma_{e.a}$) components. The van der Waals component is represented as:

$$\sigma_{VW} = \sigma_o + \sigma_p + \sigma_d + \sigma_{d.e.l} - \sigma_r,$$

---

* The authors mean forces of chemical interaction.

[1] Frantsevich Institute for Problems of Materials Science, National Academy of Sciences of Ukraine, Kiev, Ukraine; e-mail: ArRadch@ipms.kiev.ua.

Translated from Poroshkovaya Metallurgiya, Vol. 51, No. 1–2 (483), pp. 22–33, 2012. Original article submitted May 29, 2009.

where σ_o, σ_p, σ_d is the orientation, polarization, and dispersion components, respectively [5]; $\sigma_{d.e.l}$ is due to the formation of a double electric layer [6]; and σ_r is the component allowing for repulsion between molecules [7]. The mechanical component

$$\sigma_{mech} = \sigma_i + \sigma_s + \sigma_{en}$$

is represented by contributions from interlocking σ_i, seizure σ_s, and entanglement σ_{en} of particles [8].

Elastic aftereffect $\sigma_{e.a}$ of a compact differs in vertical ($\sigma_{e.a.vert}$) and horizontal or lateral ($\sigma_{e.a.lat}$) directions:

$$\sigma_{e.a.lat} = \xi\sigma_{e.a.vert},\ \sigma_{e.a.vert} = -P_c / S_{com},$$

where P_c, $\sigma_{e.a.vert}$, and $\sigma_{e.a.lat}$ are the compacting pressure and vertical and lateral stresses, respectively; ξ is the lateral pressure coefficient (from 0.2 to 0.8 [9]); and S_{com} is the area of the compact contacting with the punch.

Note that this paper does not address components σ_{el} and σ_{mag} resulting from magnetization or charging of powders. Component σ_{chem} occurs only under special deformation processing of powder blanks [4], and can be neglected in ordinary conditions of warm and cold pressing [1]. Hence, the green strength in our case is determined by molecular and mechanical components.

There are two methods to evaluate the molecular interaction between macroscopic bodies such as powders: microscopic and macroscopic [10, 11]. With the first method, the energy of interaction is determined by integrating pairwise molecular interactions, additivity of dispersion forces being taken into account. However, calculations based on adding together the energy of pair interactions have no adequate theoretical justification and can apply only to systems consisting of isolated particles, i.e., to the ideal case. With the other method, the interacting bodies are regarded as a continuum. Their interaction is due to a fluctuating electromagnetic field present inside every matter and going beyond its boundaries. This approach can apply to any bodies, regardless of their molecular nature and the distance between particles. The calculations use the Maxwell equation for the distance between particles longer than electromagnetic wavelengths of the material. The equation also accounts for delay effects. The experimental results agree well with the theory developed by Lifshitz [12].

The papers [13–16] attempt to evaluate the effect of van der Waals forces in pressing of different powders, but no calculations were performed because particle material constants were missing. The only exception was pressing of fine ZrO_2 powders, when an approximate value of the Hamaker constant was used [15].

Easterling and Thölén [13] provided only an expression for the interaction between two spherical particles:

$$f_{LW} = \frac{\hbar\omega d}{32 z_0^2}, \tag{2}$$

where $\hbar\omega$ is the Lifshitz–van der Waals constant ($\hbar$ is Planck's constant, ω is characteristic frequency of the absorption spectrum of particle material); d is the diameter of a particle; and z_0 is the shortest possible distance between two particles.

Grechka [14], with reference to Rumpf and Orr, gives only a formula (without experimental data) to calculate green tensile strength ensured by van der Waals forces:

$$\sigma_{VW(Gr)} = \frac{3A\rho_{comp}K}{64 z^2 \pi d}, \tag{3}$$

where A is the Hamaker constant depending on particle material and varying from 10^{-13} to 10^{-12} erg (10^{-20} to 10^{-19} N · m); z is the distance between two particles (<100 nm); ρ_{comp} is the compact relative density; and K is the coordination number.

To determine the strength of a compact made of ceramic equigranular powder in the absence of binder, Bortzmeyer [15] proposed the following equation:

$$\sigma_{VW(H)} = \frac{A\rho_{comp}}{24 z_0^2 (1-\rho_{comp}) d}, \tag{4}$$

where the force contributing to this strength was calculated as

$$f_{\mathrm{H}} = \frac{Ad}{24z_0^2}\,. \tag{5}$$

The strength due to van der Waals forces (~0.03 MPa) was much lower than the values obtained for compacts of fine ZrO_2 powder. Since there is no van der Waals force calculated for metal powders, we use data for pharmaceutical powders whose particles are close to metal particles in size. The strength of different pharmaceutical pills is directly proportional to the measured force of molecular interaction, which varied from 1.2 to 66 nN [16].

Van der Waals forces have not calculated for pressing of metal and nonmetal medium-size and coarse powders. In this regard, the contribution of van der Waals forces to the strength of such compacts is of particular interest.

Our goal is to determine and calculate the effect of van der Waals forces on the strength of metal and nonmetal medium-size and coarse powders and to compare the results with the tensile strength of compacts produced at different compacting pressures.

MATERIALS AND METHODS

Table 1 summarizes the properties of some powders of five metals (Al, Zn, Cu, Ni, and Mo) and one nonmetal (FeSi) [8]. The following parameters are determined for the powders: relative apparent density (RAD) as per standard DSTU 2495–94; average particle size, dry screening method (as per GOST 23402–78); and oxygen content, hydrogen reduction method (GOST 18897–98). There are also characteristic temperature (t^*), onset recrystallization temperature (t^{o}_{r}) [17]; atomic spacing (b) [18], and strength of particle material [19].

Compacts 11.3 mm in diameter and 11–14 mm in height were produced by double-ended pressing using the standard procedure to determine densification at room temperature (as per GOST 25280–90). The compacting pressure was 200, 400, 600, and 800 MPa for most powders. The green relative apparent density was determined geometrically (compacts were measured with a micrometer and weighed at a VLR-200 analytical balance). The green tensile strength was determined with an indirect method [20]. For the metals, the Lifshitz–van der Waals constants ($\hbar\omega$), taken from different sources [21, 23, 24], ranged from $2.08 \cdot 10^{-19}$ to $8.5 \cdot 10^{-19}$ N · m.

TABLE 1. Properties of Starting Powders and Particle Material

Powder material and grade	RAD	d_{av}, μm	O_2, wt.%	t^*, °C	t^{o}_{r}, °C	b, pm [18]	$A \cdot 10^{-19}$, N · m	$\hbar\omega \cdot 10^{-19}$, N · m	σ_t, MPa [19]
Zink PTs1	0.409	10	0.52–0.70	–155	53	266	–	2.08 [19]	108–392
Nickel PNK-1L6	0.119	11	0.33	<52	571	249	5.30 [20]	–	343–667
Nickel PNÉ-1	0.360	41	0.09	<52	571	249	5.30 [20]	–	343–667
Copper PMS-1	0.177	38	0.16	–22	385	255	0.65 [20]	8.50 [21]	120–235
Atomized copper	0.568	120	0.05	–22	385	255	0.65 [20]	8.50 [21]	120–235
Aluminum PA-2	0.410	180	0.25	–107	173	286	3.50 [20]	4.00 [21]	90–100
Molybdenum MPCh	0.220	25	0.21	285	1152	271	–	4.56 [22]	784–1177
FeSi (0.2–0.1)*	0.395	150	–	608	–	400	1 [13]	–	–

* The powder was produced by decomposition of cast ferrosilicon FS75; its fractional composition is shown in parentheses (mm).

EXPERIMENTAL

The following simplifications were used for approximate calculations.

- To determine the maximum van der Waals contribution to strength, atomic spacing in crystallites (*b*) [18] was used as the distance between particles; i.e., it was considered that there was no air space between particles and their surface was not covered with layers of any other molecules or chemical compounds.
- The green relative density without applied pressure corresponded to the relative apparent density of the powder and, in other cases, to the relative density of the compact after pressing.
- All powders were regarded as equigranular, with average size of particles. All particles were spherical.
- For a reference calculation, we used the Hamaker constants for our metals in combination with platinum [22] and the value for ceramic materials [15] ($1 \cdot 10^{-19}$ N · m) for FeSi, which is acceptable (Hamaker constant for Si and SiO_2 is $2.3 \cdot 10^{-19}$ and $0.853 \cdot 10^{-19}$ N · m, respectively [21]).
- To evaluate the van der Waals contribution to green strength, we took into account only the order of magnitude since, given the low accuracy of measured van der Waals forces, the orders of values match well [25].
- In analysis of green strength, the Brazilian test is not appropriate for comparison of tensile strength (break) of materials with different yield stresses because of different stress states that occur during tests, but it can be used to qualitatively compare the tendency of materials to breaking. These simplifications should not significantly affect the results.

Table 2 shows the tensile strength of powder compacts determined indirectly ($\sigma_{tl.av}$) [1], the van der Waals component calculated with the Hamaker constant ($\sigma_{VW(H)max}$ and $\sigma_{VW(Gr)}$ calculated by formulas (3) and (4), respectively) and with the Lifshitz–van der Waals constant ($\sigma_{VW(LW)max}$ by formula (3), where (2) was used instead of the force calculated by (5)), and their ratios. Note that the van der Waals component increased with compacting pressure from 0.0002 MPa for compacts from electrolytic copper powder at zero pressure to 0.36 MPa for compacts from gas-atomized copper powder at a pressure of 800 MPa.

TABLE 2. Tensile Strength Calculated for Powders by Formulas (3)–(4)

Compacting pressure, MPa	Average RAD	$\sigma_{tl.av}$, MPa*	$\sigma_{VW(H)max}$, MPa*	$\sigma_{VW(LW)max}$, MPa	$\sigma_{VW(Gr)max}$, MPa	$\sigma_{tl.av}/\sigma_{VW(H)max}$	$\sigma_{tl.av}/\sigma_{VW\,(LW)max}$	$\sigma_{tl.av}/\sigma_{VW(Gr)}$
Al								
0	0.410	σ_{VW}**	0.0010	0.0013	0.0280	1	1	1
200	0.931	2.645	0.0200	0.0253	0.0636	132	105	42
400	0.975	7.564	0.0570	0.0718	0.0665	133	105	114
600	0.981	8.486	0.0769	0.0972	0.0670	110	87	127
800	0.983	10.975	0.0877	0.1108	0.0671	125	99	163
Zn								
0	0.409	σ_{VW}	–	0.0085	–	–	1	–
200	0.837	0.060	–	0.0627	–	–	1	–
400	0.945	2.091	–	0.2090	–	–	10	–
600	0.963	4.909	–	0.3230	–	–	15	–
800	0.977	5.177	–	0.5120	–	–	10	–
$Cu_{electrolytic}$								
0	0.1770	σ_{VW}	0.0002	0.0023	0.0008	1	1	1
200	0.6910	6.934	0.0025	0.0241	0.0033	2827	288	2129
400	0.8330	17.361	0.0055	0.0538	0.0039	3165	323	4420
600	0.8920	24.989	0.0090	0.0887	0.0042	2763	281	5945
800	0.9307	30.145	0.0147	0.1443	0.0044	2048	208	6873

Table 2. Continued

Compacting pressure, MPa	Average RAD	$\sigma_{tl.av}$, MPa*	$\sigma_{VW(H)max}$, MPa*	$\sigma_{VW(LW)max}$, MPa	$\sigma_{VW(Gr)max}$, MPa	$\sigma_{tl.av}$ / $\sigma_{VW(H)max}$	$\sigma_{tl.av}$ / $\sigma_{VW (LW)max}$	$\sigma_{tl.av}$ / $\sigma_{VW(Gr)}$
$Cu_{atomized}$								
0	0.1770	σ_{VW}	0.0002	0.0023	0.0008	1	1	1
200	0.6910	6.934	0.0025	0.0241	0.0033	2827	288	2129
400	0.8330	17.361	0.0055	0.0538	0.0039	3165	323	4420
600	0.8920	24.989	0.0090	0.0887	0.0042	2763	281	5945
800	0.9307	30.145	0.0147	0.1443	0.0044	2048	208	6873
$Ni_{carbonyl}$								
0	0.119	σ_{VW}	0.0044	–	0.0166	1	–	1
200	0.550	7.2110	0.0395	–	0.0765	183	–	94
400	0.648	22.145	0.0596	–	0.0902	371	–	245
500	0.688	29.157	0.0715	–	0.0958	408	–	304
600	0.717	37.247	0.0820	–	0.0998	454	–	373
700	0.749	38.387	0.0966	–	0.1043	397	–	368
800	0.772	49.489	0.1095	–	0.1075	452	–	461
$Ni_{electrolytic}$								
0	0.360	σ_{VW}	0.0182	–	0.0501	1	–	1
200	0.652	2.3031	0.0163	–	0.0243	141	–	95
400	0.762	10.3288	0.0278	–	0.0284	371	–	363
500	0.804	12.8009	0.0355	–	0.0300	360	–	427
600	0.835	20.6760	0.0440	–	0.0312	470	–	663
700	0.864	22.8493	0.0551	–	0.0323	415	–	708
800	0.884	28.7510	0.0661	–	0.0330	435	–	871
Mo								
0	0.220	σ_{VW}	–	0.0022	–	–	1	–
200	0.590	1.7452	–	0.0112	–	–	156	–
400	0.682	6.8430	–	0.0167	–	–	410	–
600	0.766	8.8837	–	0.0254	–	–	350	–
800	0.787	17.4380	–	0.0286	–	–	609	–
FeSi								
0	0.220	σ_{VW}	0.000049	–	0.000164	1	–	1
400	0.722	0.0591	0.000451	–	0.000539	131	–	110
800	0.740	0.2044	0.000494	–	0.000552	414	–	370

* The indices "av" and "max" denote the average and maximum values for σ_t, $\sigma_{VW(H)}$, and $\sigma_{VW(LW)}$. ** Considering our simplifications, we assume that only van der Waals force acts on particles in case of loose powder: $\sigma_{tl.av} = \sigma_t = \sigma_{VW}$.

The strength changes from ~0 MPa for atomized copper powder compacts to 50 MPa for carbonyl nickel powder compacts (compacting pressure). The $\sigma_{tl.av}$ / σ_{VW} ratio at compacting pressure from 200 to 800 MPa varies from 41 for Al to 870 for $Ni_{electrolytic}$. We calculated the coordination number (K) at relative density (ρ) in the range 0.177–0.7 as [26]

$$K = \frac{1}{1-\sqrt[3]{\rho}}\ . \tag{5}$$

For $\rho > 0.7$, $K = 12$.

DISCUSSION

Compare the van der Waals forces that occur between two aluminum powder particles of the same size at the minimum possible distance between them ($b = 0.286$ nm) calculated by formulas (2) and (5) using the Lifshitz–van der Waals [13] and Hamaker [15] constants. Figure 1 shows the van der Waals forces versus the diameter of interacting particles, the distance between them being constant. Although formulas (2) and (5) to calculate the van der Waals force were derived using fundamentally different assumptions, the calculated value of f_{LW} is greater than f_H by a factor of 1.3 for all particle diameters. For interacting particles 1 μm in diameter, $f_{LW} = 0.245$ and $f_H = 0.199$ μN; for particles 500 μm in diameter, $f_{LW} = 122$ and $f_H = 97$ μN. The force calculated for particles 1 μm in size is close to the forces measured experimentally for pharmaceuticals (0.066–0.0012 μN) [16].

The adhesion strength calculated for aluminum powder by formulas (1)–(3) increases differently depending on compacting pressure (Fig. 2): $\sigma_{VW(LW)max}$ increases most intensively, $\sigma_{VW(H)max}$ increases slower, and $\sigma_{VW(Gr)max}$ hardly changes in the pressure range 200–800 MPa.

According to the notion of characteristic temperature [17], pressing of the powders in question is classified as cold (FeSi nonmetal and Mo bcc metal powders) and warm (Al, Cu, Ni fcc and Zn[1] hcp metal powders). By their properties (in particular, RAD and particle shape), the powders can also be divided into two groups: (i) spherical or near-spherical shape and high RAD (atomized Cu, Al, and Zn powders) and (ii) irregular (irregular, branched) shape and average or low RAD (carbonyl Ni, electrolytic Cu and Ni).

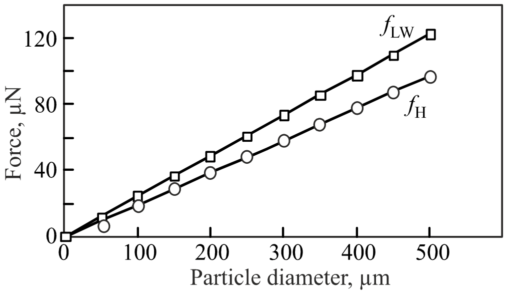

Fig. 1. The Van der Waals force calculated using the Hamaker and Lifshitz–van der Waals constants versus the diameter of aluminum powder particles

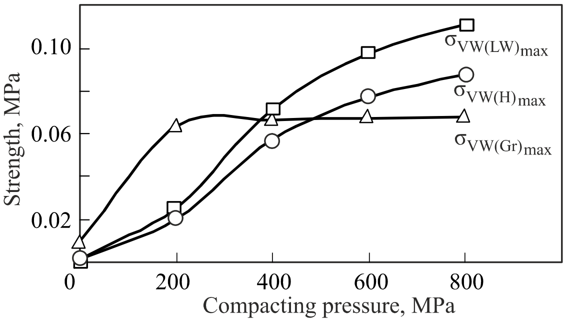

Fig. 2. The strength of aluminum powder compacts provided by van der Waals forces and calculated by formulas (3) and (4) using the Hamaker and Lifshitz–van der Waals constants versus compacting pressure

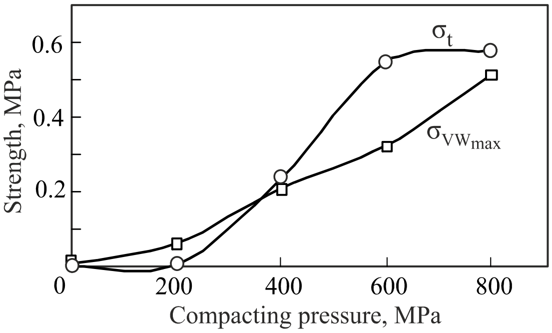

Fig. 3. The tensile strength (σ_t) and contribution of the maximum possible van der Waals force to the green strength (σ_{VWmax}) calculated by formula (4) using the Lifshitz–van der Waals constant versus compacting pressure for spherical powder PTs-1

---

[1] Forming of zinc powders at room temperature may be regarded as warm or hot depending on purity of the material, grain size, and deformation.

In the initial state and at low compacting pressures, the bonds between powder particles or the strength of compacts are mainly due to van der Waals forces, and the green strength and stress to be applied to overcome the van der Waals force practically match. However, when compacting pressure increases and the compact becomes noticeably strong (units or tens of megapascals), $\sigma_{tl.av}$ is higher than σ_{VW} by one to three orders of magnitude (Table 1). The van der Waals contribution to strength is greater than the green strength only for the atomized copper powder. To correctly evaluate the effect of molecular interaction on the green strength, the former should be compared with adhesion strength, which corresponds to tensile strength in the direction opposite to pressing (σ_t). For compact brittle materials, $\sigma_{tl} / \sigma_t = 0.9$–$1.1$ [27] (tensile strength σ_{tl} is determined indirectly), but it is not the case for green compacts made of plastic powders. For example, for the iron powder (compacts 12 mm in diameter and 8 mm in height) in the RAD range 0.7–0.93, the σ_{tl} / σ_t ratio changes from 10 to 17, i.e., by one order of magnitude at least [28]. The dependence of the σ_{tl} / σ_t ratio on the parameters of plastic metal powders has hardly been studied, so we assume that $\sigma_t \cong 0.1\ \sigma_{tl}$ for an approximate evaluation. On this basis, adhesion strength (σ_t) of zinc powder compacts, provided that there is no elastic aftereffect, can be provided only by the van der Waals component (Fig. 3). This is quite possible for zinc because the compacting temperature is close to the onset recrystallization temperature (t^o_r ~75°C), t^o_r decreasing with higher strain; moreover, local heating may occur in deformation areas.

For the copper powder with spherical particles, the onset recrystallization temperature is much higher than the compacting temperature ($t^o_r \approx 405$°C), and the elastic aftereffect in pressing is greater than the van der Waals contribution to strength ($\sigma_{mech} = 0$ and $\sigma_{e.a} >> \sigma_m$ (1)). The aluminum powder, similar to the copper powder, has $\sigma_{tl.av}$ twice as high as σ_{VW}, which can be attributed to the mechanical component originating from the penetration of solid oxide films into adjacent particles. This assumption can be confirmed by fractography of compacts [29]. Powders with branched particles show $\sigma_{tl.av}$ that is two to three orders higher than the van der Waals strength, and σ_t, considering [28], is greater by one to two orders (for warm pressing and branched particles). The maximum van der Waals strength constitutes 0.1–0.01 of the green tensile strength in the direction opposite to pressing.

Using homological compacting temperature (Θ_c) compared with ductile–brittle temperature (Θ^*) and onset recrystallization temperature (Θ^o_r) of particle material, we analyzed how temperature at which the powders were formed influenced the $\sigma_{tl.av} / \sigma_{VW}$ ratio. For the metals, we accepted $\Theta^* \cong 0.2$ (taking into account that $\Theta^* << 0.2$ for fcc metals) and $\Theta^o_r = 0.5$. Note that the homological compacting temperature induces (($\Theta_c < \Theta^o_r$) and ($\Theta_c < \Theta^*$)) or does not induce (($\Theta_c > \Theta^o_r$) and ($\Theta_c < \Theta^*$)) elastic aftereffect and plasticity in particle material. For the metal powders with spherical particles, $\Theta_c = 0.216$ for $Cu_{atomized}$ (fcc)[2], i.e., $\sigma_{tl.av} < \sigma_{VW}$; $\Theta_c = 0.432$ for Zn (hcp)[3], i.e., $\sigma_{tl.av} \approx \sigma_{VW}$; and $\Theta_c = 0.314$ for Al (fcc)[3], i.e., $\sigma_{tl.av} > \sigma_{VW}$.

For the metal powders with nonspherical particles, $\Theta_c = 0.216$ for $Cu_{electrolytic}$ (fcc)[3], i.e., $\sigma_{tl.av} >> \sigma_{VW}$; $\Theta_c = 0.170$ for $Ni_{carbonyl}$ and $Ni_{electrolytic}$ (fcc)[3], i.e., $\sigma_{tl.av} >> \sigma_{VW}$; $\Theta_c = 0.101$ for Mo (bcc)[4], i.e., $\sigma_{tl.av} > \sigma_{VW}$.

For the nonmetal FeSi[4] powder with nonspherical particles, $\Theta_c = 0.195$ and $\Theta^* \cong 0.6$–0.8, i.e., $\sigma_{tl.av} > \sigma_{VW}$. The absolute value of $\sigma_{tl.av}$ for the compact is two orders lower than for the metal powders with branched particles.

The σ_p / σ_{VW} ratio for the Mo powder should be explained: it is practically identical with that for the Ni powder, though $\Theta_c < \Theta^*$ for molybdenum. This is because characteristic temperature is always higher than cold-brittleness temperature, which can be determined using the Ioffe–Orowan scheme [30]. However, its value for chemically pure metals still has not been introduced into academic use since it depends on the purity of metals and on testing conditions and other factors. Given the nature of mechanical component, σ_{tl} is influenced by increased strength of Mo particle material (784–1177 MPa) compared with Ni powder (343–667 MPa).

---

[2] Plasticity and elastic aftereffect are present in particle material.

[3] Green compact is influenced by plasticity, elastic aftereffect, and hard oxide coating (0.25 wt.% O_2).

[4] Plasticity and elastic aftereffect are absent.

We have calculated the maximum green strength governed by the van der Waals force σ_m (1) (it is much lower than elastic aftereffect ($-\sigma_{e.a}$)). In addition, elastic aftereffect (stresses that occur in the compact are equal to stresses induced during pressing) may increase the distance between particles (decreasing molecular forces) and destroy single contacts [31]. It is clear that only the mechanical component, mechanical interlocking, can resist such great stresses; otherwise (in case of atomized copper powder), the compact just falls apart.

CONCLUSIONS

The van der Waals contribution to the strength of compacts made of medium-size and coarse metal and nonmetal powders produced at different temperatures has been calculated for the first time. This allowed us to evaluate its contribution to actual strength.

The ratio of the van der Waals force calculated using the Lifshitz–van der Waals constant to the force calculated using the Hamaker constant for two identical spherical aluminum particles (1–500 μm in diameter) is 1.3.

The van der Waals component of the green strength calculated by three different methods for aluminum powders differs from the experimentally determined green strength by three times (corresponding to compacting pressure 200 MPa).

The comparison of the $\sigma_{tl.av} / \sigma_{VW}$ ratios has shown that $\sigma_{tl.av}$ and σ_{VW} are of one order of magnitude for the zinc powder; $\sigma_{VW} > \sigma_{tl.av}$ for the atomized copper powder, though $\sigma_{tl.av}$ is greater than σ_{VW} by two to three orders for most powders; and $\sigma_{tl.av}$ is greater than σ_{VW} by one to two orders for plastic metals according to [28]. This great difference between $\sigma_{tl.av}$ and σ_{VW} can be attributed only to the effect of particle shape and mechanical interlocking [16] or seizure of particles when compacted. In fact, the powders of $\mathrm{Cu}_{\mathrm{atomized}}$ ($\sigma_{tl.av} < \sigma_{VW}$) and Zn ($\sigma_{tl.av} = \sigma_{VW}$) have spherical particles, Al ($\sigma_{tl.av} > \sigma_{VW}$) near-spherical particles, and other powders ($\sigma_{tl.av} >> \sigma_{VW}$) irregular particles.

To predict the green strength, both the shape of particles (or relative apparent density of the powder) and temperature of the particle material (homological temperature in pressing, homological characteristic temperature, and recrystallization temperature) need to be taken into account.

ACKNOWLEDGEMENTS

The thanks are due to Professor Skorokhod, Academician of the National Academy of Sciences, for valuable comments made during discussion of the paper.

REFERENCES

1. A. K. Radchenko, “Mechanical properties of green compacts. II. Effect of powder relative bulk density on the strength of compacts with different forming temperature conditions,” *Powder Metall. Met. Ceram.*, **43**, No. 11–12, 552–563 (2004).
2. W. B. Pietsch, “Adhesion and agglomeration of solids during storage, flow, and handling: A survey,” *Trans. ASME, J. Eng. Indust., Ser. B*, **5**, No. 2, 435-449 (1969).
3. A. D. Zimon and E. I. Andrianov, *Self-adhesion of Loose Materials* [in Russian], Metallurgiya, Moscow (1978), p. 288.
4. B. Yu. Dorofeev, V. Yu. Dorofeev, Yu. N. Ivashchenko, et al., “Processes of splicing in hot-molded iron base materials. I. Method of investigation and general characteristic of fractograms,” *Powder Metall. Met. Ceram.*, **27**, No. 6, 434–437 (1988).
5. N. D. Sokolov, *Molecular Interactions: Chemical Encyclopedia* [in Russian], Vol. 3, Moscow (1992), pp. 12–14.
6. B. V. Deryagin, N. A. Krotova, and V. P. Smigla, *Adhesion of Solids* [in Russian], Nauka, Moscow (1973), p. 280.
7. C. J. van Oss, M. K. Chaudhury, and R. J. Good, “Interfacial Lifshitz–van der Waals and polar interactions in macroscopic systems,” *Chem. Rev.*, **88**, 927–941 (1988).

8. M. Yu. Bal'shin, *Powder Metallurgy* [in Russian], Metallurgiya, Moscow (1948), p. 286.
9. G. A. Vinogradov and I. D. Radomysel'skii, *Pressing and Rolling of Metal Ceramic Materials* [in Russian], Mashgiz, Moscow–Kiev (1963), p. 200.
10. R. Winterton, "Van der Waals forces," *Usp, Fiz. Nauk*, **105**, No. 2, 307–320 (1971).
11. Yu. S. Barash, *Van der Waals Forces* [in Russian], Nauka, Moscow (1988), p. 344.
12. B. V. Deryagin, I. I. Abrikosova, and E. M. Lifshitz, "Molecular attraction of condensed bodies," *Usp. Fiz. Nauk*, **64**, No. 3, 495–528 (1958).
13. K. E. Easterling and A. R. Thölén, "Surface energy and adhesion at metal contacts," *Acta Metall.*, **20**, No. 8, 1001–1008 (1972).
14. V. D. Grechka, "Effect of intermolecular and electrostatic cohesive forces on the process of densification of particulate materials," *Powder Metall. Met. Ceram.*, **15**, No. 11, 830–832 (1976).
15. D. Bortzmeyer, "Tensile strength of ceramic powders," *J. Mater. Sci.*, **27**, No. 12, 3305–3308 (1992).
16. Q. Li, V. Rudolph, B. Weigl, and A. Earl, "Interparticle van der Waals force in powder flowability and compactibility," *Int. J. Pharmaceutics*, **280**, 77–93 (2004).
17. V. I. Trefilov, Yu. V. Mil'man, and I. V. Gridneva, "Role of plastic deformation in sintering covalent crystals (review)," *Powder Metall. Met. Ceram.*, **33**, No. 7–8, 357–365 (1994).
18. M. A. Shtremel', *Strength of Alloys. Lattice Defects* [in Russian], Mosk. Inst. Stali Splavov, Moscow (1999), p. 384.
19. L. V. Tikhonov, V. A. Kononenko, G. I. Prokopenko, and V. A. Rafalovskii (eds.), *Structure and Properties of Metals and Alloys: Handbook. Mechanical Properties of Metals and Alloys* [in Russian], Naukova Dumka, Kiev (1986), p. 568.
20. V. G. Osipov, "Determining the strength of compact from metal powders," *Zavod. Lab.*, **26**, No. 1, 122–125 (1960).
21. C.-J. Tsai, D. Y. H. Pui, and B. Y. H. Liu, "Elastic flattening and particle adhesion," *Aerosol Sci. Tech.*, **15**, No. 4, 239–255 (1991).
22. G. V. Dedkov, E. G. Dedkova, R. I. Tegaev, and Kh. B. Khokonov, "Measurement of van der Waals and electrostatic forces in contacts of atomic force microscope probe with metal surfaces," *Pis'ma Zh. Tekh. Fiz.*, **34**, No. 1, 38–47 (2008).
23. Y. H. Addab, "Conception et réalisation d'un système de micromanipulation contrôlé en effort et en position pour la manipulation d'objets de taille micrométrique," *Thèse de Doctorat*, L'Université de Franche-Comté, Besançon (2000), p. 189.
24. R. V. Brach and P. F. Dunn, "A mathematical model of the impact and adhesion of microspheres," *Aerosol Sci. Tech.*, **16**, No. 1, 51–64 (1992).
25. A. W. Adamson, *Physical Chemistry of Surfaces*, John Wiley and Sons, New York (1976).
26. R. M. German, *Powder Metallurgy Science*, Metal Powder Industries Federation, New Jersey, Princeton (1984), 279.
27. V. V. Glagolev and A. G. Lanin, "Assessing the strength of elastic materials with the diametric compression method," in: *Methods for Study of Refractory Materials* [in Russian], Atomizdat, Moscow (1970), pp. 148–156.
28. P. Doremus, F. Toussaiht, and O. Alvain, "Simple tests standard procedure for the characterization of green compacted powder," in: A. Zavaliangos and A. Laptev (eds.), *Recent Developments in Computer Modeling of Powder Metallurgy Processes*, IOS Press, Amsterdam (2001), pp. 282–293.
29. M. Strömgren, H. Aström, and K. Easterling, "The effect of interparticle contacts area on the strength of cold-pressed aluminum powder compacts," *Powder Met.*, **16**, No. 32, 155–165 (1973).
30. V. M. Mishin, I. V. Kislyuk, and V. I. Sarrak, "Analyzing the effect of alloying on iron cold-shortness threshold in terms of the Ioffe–Orowan scheme," *Fiz. Met. Metalloved.*, No. 7, 188–192 (1991).
31. V. N. Antsiferov and V. E. Perel'man, *Compaction Mechanics of Powder and Composite Materials* [in Russian], Graal Publishing House, Moscow (2001), p. 628.